2023

Longitudinal trajectories of basal forebrain volume in normal aging and Alzheimer's disease

Ying Xia

Paul Maruff

Vincent Doré

Pierrick Bourgeat

Simon M. Laws
Edith Cowan University

See next page for additional authors

10.1016/j.neurobiolaging.2023.09.002
Xia, Y., Maruff, P., Doré, V., Bourgeat, P., Laws, S. M., Fowler, C., . . . Fripp, J. (2023). Longitudinal trajectories of basal forebrain volume in normal aging and Alzheimer's disease. Neurobiology of Aging, 132, 120-130. https://doi.org/10.1016/j.neurobiolaging.2023.09.002

Neurobiology of Aging 132 (2023) 120–130

Contents lists available at ScienceDirect

Neurobiology of Aging

journal homepage: www.elsevier.com/locate/neuaging.org

Regular article

Longitudinal trajectories of basal forebrain volume in normal aging and Alzheimer's disease

Ying Xia [a,*], Paul Maruff [b,c], Vincent Doré [d,e], Pierrick Bourgeat [a], Simon M. Laws [f,g,h], Christopher Fowler [c], Stephanie R. Rainey-Smith [i,j,k,l], Ralph N. Martins [j,l,m], Victor L. Villemagne [d,g,n], Christopher C. Rowe [d,o], Colin L. Masters [c], Elizabeth J. Coulson [p,q], Jurgen Fripp [a]

[a] The Australian e-Health Research Centre, CSIRO Health and Biosecurity, Brisbane, Queensland, Australia
[b] Cogstate Ltd, Melbourne, Victoria, Australia
[c] The Florey Institute of Neuroscience and Mental Health, The University of Melbourne, Parkville, Victoria, Australia
[d] Department of Nuclear Medicine and Centre for PET, Austin Health, Melbourne, Victoria, Australia
[e] The Australian e-Health Research Centre, CSIRO Health and Biosecurity, Melbourne, Victoria, Australia
[f] Collaborative Genomics and Translation Group, School of Medical and Health Sciences, Edith Cowan University, Joondalup, Western Australia, Australia
[g] Centre for Precision Health, Edith Cowan University, Joondalup, Western Australia, Australia
[h] Curtin Medical School, Curtin University, Bentley, Western Australia, Australia
[i] Centre for Healthy Ageing, Health Futures Institute, Murdoch University, Murdoch, Western Australia, Australia
[j] Australian Alzheimer's Research Foundation, Sarich Neuroscience Research Institute, Nedlands, Western Australia, Australia
[k] School of Psychological Science, University of Western Australia, Crawley, Western Australia, Australia
[l] School of Medical and Health Sciences, Edith Cowan University, Joondalup, Western Australia, Australia
[m] Department of Biomedical Sciences, Macquarie University, Sydney, New South Wales, Australia
[n] Department of Psychiatry, University of Pittsburgh, Pittsburgh, PA, USA
[o] Florey Department of Neuroscience and Mental Health, The University of Melbourne, Parkville, Victoria, Australia
[p] Queensland Brain Institute, The University of Queensland, Brisbane, Queensland, Australia
[q] School of Biomedical Sciences, The University of Queensland, Brisbane, Queensland, Australia

ARTICLE INFO

Article history:
Received 23 February 2023
Revised 3 August 2023
Accepted 7 September 2023
Available online 11 September 2023

Keywords:
Alzheimer's disease
Amyloid-β
Basal forebrain
Longitudinal
Magnetic resonance imaging

ABSTRACT

Dysfunction of the cholinergic basal forebrain (BF) system and amyloid-β (Aβ) deposition are early pathological features in Alzheimer's disease (AD). However, their association in early AD is not well-established. This study investigated the nature and magnitude of volume loss in the BF, over an extended period, in 516 older adults who completed Aβ-PET and serial magnetic resonance imaging scans. Individuals were grouped at baseline according to the presence of cognitive impairment (CU, CI) and Aβ status (Aβ−, Aβ+). Longitudinal volumetric changes in the BF and hippocampus were assessed across groups. The results indicated that high Aβ levels correlated with faster volume loss in the BF and hippocampus, and the effect of Aβ varied within BF subregions. Compared to CU Aβ+ individuals, Aβ-related loss among CI Aβ+ adults was much greater in the predominantly cholinergic subregion of Ch4p, whereas no difference was observed for the Ch1/Ch2 region. The findings support early and substantial vulnerability of the BF and further reveal distinctive degeneration of BF subregions during early AD.

Abbreviations: AIBL, Australian Imaging, Biomarkers and Lifestyle; *APOE*, apolipoprotein E; BF, basal forebrain; BFV, basal forebrain volume; CDR, clinical dementia rating; CL, Centiloid; Ch1/Ch2, the medial septal nucleus and vertical limb of the diagonal band of Broca; Ch4p, the posterior subdivision of the nucleus basalis of Meynert; CI, cognitively impaired; CSF, cerebrospinal fluid; CU, cognitive unimpaired; FDR, false discovery rate; GM, gray matter; HV, hippocampal volume; LMM, linear mixed-effects model; MMSE, mini-mental state examination; ROI, region of interest; SD, standard deviation; TIV, total intracranial volume; WM, white matter.

* Corresponding author at: Surgical Treatment and Rehabilitation Service–STARTS, Level 7, 296 Herston Road, Herston, Queensland 4029, Australia.
E-mail address: ying.xia@csiro.au (Y. Xia).

https://doi.org/10.1016/j.neurobiolaging.2023.09.002

1. Introduction

In humans, the cholinergic basal forebrain (BF) system provides the major cholinergic innervation to cerebral cortex, thereby directly influencing aspects of cognition such as memory, attention, and executive function (Ballinger et al., 2016; Prado et al., 2017). Alzheimer's disease (AD) is a neurodegenerative disease characterized by abnormal accumulation of amyloid-β (Aβ) and hyperphosphorylated tau, leading to neuronal loss, memory and cognitive impairment, and ultimately dementia. Biomarkers of Aβ and tau levels now allow detection of AD many years before the onset of dementia, providing an important window for understanding disease etiology (Villemagne et al., 2013). Initial models of AD pathophysiology, and consequent pharmacotherapies, focused on the observed disruption to cholinergic neurotransmission due to the neuronal degeneration (Francis et al., 1999). Recent studies suggest complex interactions between cholinergic degeneration and AD pathology, where Aβ itself is toxic to cholinergic neurons in the BF and loss of cholinergic neurons may also accelerate accumulation of Aβ and tau (Hampel et al., 2018; Ramos-Rodriguez et al., 2013; Schliebs, 2005). Hence, Aβ-related neuronal death could be biased toward cholinergic neurons in the BF, which then reduces their regulation of attentional and memory networks that center on the hippocampus and cortex (Mesulam, 1998).

Although the cholinergic BF neurotransmission system can be assessed directly using in vivo positron emission tomography (PET) imaging (Bohnen et al., 2018; Xia et al., 2022), volumetric magnetic resonance imaging (MRI) assessments of the BF are also validated as a surrogate marker of cholinergic degeneration (Kilimann et al., 2014; Teipel et al., 2005). Many cross-sectional studies show that, compared to age-matched adults without AD, BF volumes (BFVs) are reduced substantially across the preclinical and clinical AD stages (Grothe et al., 2012; Scheef et al., 2019). Reduced BFVs are also associated with a positive response to therapy with acetylcholinesterase inhibitors (Müller et al., 2021). In both preclinical and clinical stages of AD, higher Aβ levels are associated moderately with lower BFV (Grothe et al., 2014; Kerbler et al., 2015; Teipel et al., 2014). Furthermore, there is growing evidence for a specific vulnerability of cholinergic BF cell groups to AD pathologies (Brauer et al., 1991; Geula et al., 2021) with the Aβ-related atrophy in the BF more pronounced in the posterior subdivision of the nucleus basalis of Meynert (Ch4p) at the preclinical and prodromal stages (Cantero et al., 2017, 2020; Grothe et al., 2012). The neuronal loss then proceeds anteriorly to include all BF nuclei when symptomatic dementia becomes overt (Grothe et al., 2012).

Although data from cross-sectional comparisons can be informative regarding the presence of disease, longitudinal studies allow a more thorough understanding of the nature and magnitude of volume loss in the BF as AD develops. However, as biological changes that characterize predementia AD can occur over decades, extended study periods are necessary to understand the nature and timing of any Aβ-related volume loss in the BF. Although several longitudinal studies have shown changes in BFV in aging and AD, these were restricted to a specific stage of the disease (i.e., preclinical or prodromal AD) and conducted over short time frames (i.e., 2 or 3 years) (Cavedo et al., 2020; Grothe et al., 2013; Schmitz et al., 2016, 2018). Therefore, although these studies provide a basis for modeling the interaction between Aβ and BF degeneration, further studies conducted over a longer time period, including samples with varying degrees of clinical disease severity, are necessary to fully understand cholinergic BF degeneration over the course of the disease.

The aim of this study was to investigate the nature and magnitude of volume loss in the BF and hippocampus over periods up to 14 years across the AD spectrum, including normal aging, preclinical, and symptomatic AD. The present study utilized a large sample of older individuals with well-characterized clinical disease status and AD biomarker levels to examine the longitudinal patterns of volumetric change in the BF and hippocampus and to distinguish differences in volume loss trajectories between BF subregions across different stages of AD.

2. Material and methods

2.1. Participants

Five hundred sixteen participants aged over 60 years were selected from the Australian Imaging, Biomarker and Lifestyle (AIBL) study of ageing. Information regarding the study protocol, exclusion criteria, recruitment, and diagnostic criteria has been described elsewhere (Ellis et al., 2009; Fowler et al., 2021). Briefly, participants underwent comprehensive imaging, biomarker, and clinical assessment at 18-month intervals. Ethics approval for the AIBL study was obtained from the institutional ethics committees of Austin Health, St Vincent's Health, Hollywood Private Hospital, and Edith Cowan University. Written informed consent was obtained from all participants before participation and at each visit.

Participants were selected for this study on the basis that they had undergone Aβ-PET imaging, MRI assessment, and cognitive assessment on the same time visit (referred to as the baseline visit), followed by repeated MRI assessments on at least 1 follow-up visit. Of these 516 participants at baseline, 40 participants met National Institute of Neurological and Communicative Disorders and Stroke/Alzheimer's Disease and Related Disorders Association criteria (McKhann et al., 1984) for AD diagnosis, 62 had mild cognitive impairment (Petersen et al., 1999), and 414 were individuals without cognitive impairment. The carriage of the apolipoprotein E (*APOE*) ε4 allele was determined for all participants as previously described (Fowler et al., 2021).

At the baseline assessment, the clinical dementia rating (CDR) and mini-mental state examination scores were collected. The CDR score evaluates 6 domains of function (memory, orientation, problem-solving, home and hobbies, community affairs, and self-care) and provides a staging system to assess participants' comprehensive cognitive levels, which indicates whether dementia is absent (CDR = 0), questionable (CDR = 0.5), mild (CDR = 1), moderate (CDR = 2), or severe (CDR = 3) (Morris, 1993). In this study, participants with moderate-to-severe dementia severity (CDR > 1) at baseline were excluded. The clinical dementia severity stage of each participant was determined from CDR scores at baseline, where participants with CDR scores of 0.5 or 1 were classified as cognitively impaired (CI) and those with CDR = 0 were CU.

2.2. Brain imaging

Aβ PET imaging at baseline has been performed using 4 different radiotracers: ^{11}C-Pittsburgh compound-B (PiB, 53.3%), ^{18}F-flutemetamol (28.1%), ^{18}F-florbetapir (14.5%), and ^{18}F-NAV4694 (4.1%). The PET imaging methods for different tracers have been previously described (Clark et al., 2011; Rowe et al., 2010; Vandenberghe et al., 2010).

MRI scans were acquired at 3 Australian scanning centers, 2 in Melbourne using Siemens 3T Trio (50.1% of scans), Siemens 3T Skyra (14.2%), and Siemens 3T Prisma Fit (2.9%) scanners, and 1 in Perth using Siemens 3T Verio (18.8%) and Siemens 1.5 T Avanto (14.0%) scanners. A 3D T1-weighted magnetization-prepared rapid gradient-echo sequence was acquired, which mainly (88.8%) used parameters: repetition time = 2300 ms, echo time = 2.98 or 3.05 ms, flip angle = 9°, voxel size 1.2 × 1 × 1 mm^3 or 1 × 1 × 1 mm^3.

2.3. Imaging data processing

2.3.1. Aβ PET assessment

Aβ burden was quantified automatically from PET scans using CapAIBL (Bourgeat et al., 2015) and estimated in terms of Centiloid values with nonnegative matrix factorization-based quantification (Bourgeat et al., 2021). Abnormal levels of Aβ burden (Aβ+) were determined with a threshold of 20 Centiloid, which has been validated using autopsy data (Doré et al., 2019).

2.3.2. Longitudinal structural MRI processing

The overview of the longitudinal MRI segmentation workflow is detailed in Supplementary Fig. 1. First, a longitudinal segmentation pipeline in the computational anatomy toolbox was used to process the longitudinal structural MRI, with the aging workflow applied to account for inevitable age-related changes over time (Gaser et al., 2022). In brief, for each participant, MRI scans from all visits were rigidly aligned, and an average (midpoint) image was calculated and segmented into gray matter (GM), white matter, and cerebrospinal fluid. A subject-specific tissue probability map was then created based on the segmentation of the average image, which was used to segment each time-point-specific MRI. Both the total intracranial volumes and hippocampal volumes (HV) were calculated from the final brain segmentations of MRI for all visits, with the bilateral hippocampal regions identified using the Neuromorphometrics atlas (https://www.neuromorphometrics.com).

To identify the BF region, the average (midpoint) GM and white matter segmentations were first registered to a pregenerated population template using the DARTEL toolbox (Ashburner, 2007). The resulting deformation map was then used to warp all time-point-specific GM segmentations into the template space. The warped GM segmentations were further modulated and smoothed with a 4 mm Gaussian kernel. The population template used in this study was created from a subset of 291 CU participants from the AIBL study, who were identified as having CDR = 0, mini-mental state examination ≥ 29, and stable Aβ− status. For any participant with longitudinal MRI available, the average (midpoint) segmentations were used in the template creation. The BF region of interest (ROI) was identified in the template space using a stereotactic mask of the bilateral BF, as illustrated in Supplementary Fig. 1, which was created based on a combination of postmortem MRI and histology from an autopsy brain (Kilimann et al., 2014). This BF mask was divided into 6 subregions, including the medial septal nucleus and vertical limb of the diagonal band of Broca (Ch1/Ch2), the nucleus of horizontal limb of the diagonal band of Broca (Ch3), Ch4p, anterior and intermediate parts of the nucleus basalis of Meynert (Ch4a_i), nucleus subputaminalis, and the juxta-commisural cell cluster. The total BFV was calculated as the sum of voxel intensities from the smoothed GM images within these subregions. Considering the small size and colocation of the BF cholinergic system, volumetric measures of all 6 BF subregions may show similar changes over time, which increases the risk of type I error. In this study, we focused only on 2 BF subregions, Ch1/Ch2 and Ch4p, which have been suggested to exhibit different vulnerabilities to AD pathology (Scheef et al., 2019; Schmitz et al., 2018).

2.4. Statistical analysis

Participants were grouped at their baseline clinical assessment according to the presence of cognitive impairment (CU or CI) and Aβ status (Aβ−, Aβ+), which provided 4 groups: CU Aβ−, CU Aβ+, CI Aβ−, and CI Aβ+. Group-wise differences were assessed with 1-way analysis of variance tests for continuous data and χ^2 testing for categorized data.

For all volumetric measures, the effects of the multiscanner were first harmonized using the longitudinal ComBat method (Beer et al., 2020), accounting for fixed effects of age at baseline, sex, clinical diagnosis, time, and their interaction diagnosis × time. The harmonized volumes were then adjusted for total intracranial volume using the regression coefficients estimated from the CU Aβ− group and further transformed into standardized scores using the mean and standard deviation (SD) of the baseline measures in the CU Aβ− group. This allowed for direct comparison of the magnitude of change over time across different ROIs. The distribution of volumetric measures for different ROIs in the CU Aβ− group did not deviate from symmetry, as their skewness values were all between −0.5 and 0.5.

2.4.1. Cross-sectional analysis

Baseline measures for HV, BFV, and then for Ch4p and Ch1/Ch2 were compared across groups using analysis of covariance with post-hoc pairwise comparisons. Age, sex, and education were included as covariates. Multiple pairwise comparisons were corrected using the Benjamin-Hochberg false discovery rate method. $p < 0.05$ was considered statistically significant. The effect size of an independent variable in the analysis of covariance model was measured using the partial eta-squared (η^2), where an effect size of 0.01 is small, 0.06 is medium, and 0.14 is large (Cohen, 1973).

2.4.2. Longitudinal analysis

Longitudinal analyses were conducted to compare the trajectories of change in BFV and HV between groups, in which standardized scores for BFV, HV, and BF subregional volumes across all repeated visits were submitted as dependent variables to a series of group (CU Aβ−, CU Aβ+, CI Aβ+, CI Aβ−) linear mixed-effects models (LMM). In each LMM, time from the baseline (in years), group, and their interaction group × time were entered as fixed factors. Participant and time from the baseline were included as random factors. Age at baseline, sex, education, and *APOE* ε4 carriage were entered as covariates. The test of the main hypothesis that the rates of volume loss would be different between groups was determined by the presence of a significant group-by-time interaction term. Where this occurred, a series of planned interaction contrasts constructed within the LMM were applied to compare the trajectory of volume loss in the CU Aβ− group to that in the CU Aβ+, CI Aβ+, and CI Aβ− groups, while continuing to control for covariates. The magnitude of group-wise differences in rates of volume loss was assessed using Cohen's *d*.

Additionally, the post-hoc analysis was conducted to determine the effect of Aβ burden at baseline on rates of volume loss in the entire and subregional BF and hippocampus among CU and CI older individuals. For a better interpretation of volumetric changes over time across different regions, annual percentage change (in %/y) was calculated based on the rates of decline estimated from LMM divided by the baseline volumetric measures.

3. Results

3.1. Clinical and demographic characteristics

Participants in the AIBL study (N = 516) were monitored over an average of 5.0 (SD = 3.1) years with 314 (60.9%) completing MRI on at least 3 visits (6.6 ± 2.8 years) and the remainder completing MRI on 2 visits (2.6 ± 1.7 years). Based on the baseline clinical dementia severity and Aβ status, 288 (55.8%) participants were classified as CU

Table 1
Baseline cohort characteristics

	CU Aβ−	CU Aβ+	CI Aβ+	CI Aβ−	p[a]
Number of participants	288	101	86	41	-
Baseline age (years)	71.6 ± 5.7	75.1 ± 6.3	74.6 ± 6.3	74.3 ± 6.6	< 0.001
Follow-up (years)	5.7 ± 3.1	4.6 ± 3.0	3.3 ± 2.1	5.0 ± 3.3	< 0.001
Sex (F, %)	171 (59.4%)	51 (50.5%)	44 (51.2%)	12 (29.3%)	0.003
Education (≥12 y, %)	160 (55.6%)	59 (58.4%)	40 (46.5%)	20 (48.8%)	0.325
Body mass index	26.6 ± 4.1	25.9 ± 3.7	25.4 ± 4.5	26.1 ± 4.1	0.099
Hypertension (%)	97 (33.7%)	41 (40.6%)	34 (39.5%)	18 (43.9%)	0.383
Diabetes (%)	19 (6.6%)	7 (6.9%)	5 (5.8%)	5 (12.2%)	0.549
MAP, mm Hg	97.1 ± 11.3	99.3 ± 11.1	98.2 ± 11.6	99.2 ± 9.2	0.353
APOE ε4 carrier (%)	57 (19.8%)	51 (50.5%)	59 (68.6%)	7 (17.1%)	< 0.001
MMSE	28.9 ± 1.1	28.6 ± 1.4	24.7 ± 4.0	27.7 ± 2.0	< 0.001
No. of CDR = 1 (%)	0	0	20 (23.3%)	2 (4.9%)	-
Aβ burden (Centiloids)	0.8 ± 7.2	57.6 ± 26.2	86.6 ± 28.1	0.4 ± 7.1	< 0.001

MAP calculated as (systolic blood pressure + 2 × diastolic blood pressure)/3.
Key: Aβ, amyloid-beta; CDR, clinical dementia rating; CI, cognitively impaired; CU, cognitively unimpaired; MAP, mean arterial pressure; MMSE, mini-mental state examination.
[a] The *p* values were calculated using 1-way ANOVA tests for continuous data or χ^2 testing for categorical data.

Aβ−, 101 (19.6%) as CU Aβ+, 86 (16.7%) as CI Aβ+, and 41 (7.9%) as CI Aβ−. The distribution of participants that completed MRI on 2, 3, or more visits across the 4 clinical groups is provided in Supplementary Table 1. The demographic and clinical characteristics at baseline across groups are summarized in Table 1. Compared to the CU Aβ+ and CI Aβ+ groups, individuals in the CU Aβ− group were younger with longer follow-up periods. Carriage of the *APOE* ε4 allele was greatest in the CI Aβ+ group (68.6%) and lowest in the CI Aβ− group (17.1%).

3.2. BF and hippocampal volumes at first visit

At baseline, significant group effects were identified for the total BFV and HV as well as BF subregional volumes (Fig. 1). Pairwise group comparisons showed smaller BFV and HV for the CI Aβ+ group compared with other 3 groups, with medium-to-large effect sizes. No significant difference between the CU Aβ− and CU Aβ+ groups was observed for BFV or HV. Compared to the CU Aβ− group, the CI Aβ− group had a smaller HV with a small effect size (η^2 = 0.01), whereas no differences were noted for BFV.

For the BF subregions, the CI Aβ+ group showed smaller Ch4p volumes compared with CU groups, with large effect sizes (η^2 = 0.31 and 0.25), while these group differences in Ch1/Ch2 volumes were much smaller (η^2 = 0.04 and 0.05). Significant differences in Ch4p volumes were also observed between the CU Aβ− and CU Aβ+ groups (η^2 = 0.01) as well as between the CI Aβ− and CI Aβ+ groups (η^2 = 0.15), whereas no differences were noted for Ch1/Ch2 volumes.

3.3. Trajectory of change in BF and hippocampal volumes

For the total BFV, the group × time interaction from LMM was significant (F = 28.71, p < 0.001). The CU Aβ− group showed a rate of BFV loss of −0.066 ± 0.010 SD per year (∼−0.50%/y), while the CU Aβ+ and CI Aβ+ groups exhibited a greater average rate of −1.75 and −2.12%/y (Supplementary Table 2). The interaction contrasts between groups in Table 2 indicated that, compared to the CU Aβ− group, the magnitude of BFV loss was significantly greater in the CU Aβ+ (Cohen's d = 1.20), CI Aβ+ (Cohen's d = 1.53), and CI Aβ− (Cohen's d = 0.51, p = 0.009) groups. Comparing the CU Aβ+ and CI Aβ+ groups revealed no significant difference in the rate of the total BFV loss (Cohen's d = 0.18, p = 0.266). The trajectories of BFV loss in different groups are illustrated in Fig. 2A.

For HV, the group × time interaction from LMM was significant (F = 73.40, p < 0.001). The CU Aβ− group showed a rate of HV loss of −0.091 ± 0.007 SD per year (∼−0.74%/y), while the CU Aβ+ and CI Aβ+ groups exhibited a greater average rate of −1.97 and −3.27%/y. The interaction contrasts between groups indicated that, compared to the CU Aβ− group, the magnitude of HV loss was significantly greater in the CU Aβ+ and CI Aβ+ groups (Cohen's d = 1.02 and 1.85), but not in the CI Aβ− group (Cohen's d = 0.21, p = 0.398). The CI Aβ+ group showed a greater rate of HV loss (Cohen's d = 0.61) compared to the CU Aβ+ group. The trajectories of HV loss in different groups are illustrated in Fig. 2B.

For Ch4p, the group × time interaction from LMM was significant (F = 39.60, p < 0.001). The CU Aβ− group showed a rate of Ch4p volume loss of −0.078 ± 0.006 SD per year (∼−0.72%/y), while the CU Aβ+ and CI Aβ+ group exhibited a greater average rate of −1.54 and −2.74%/y. The interaction contrasts between groups indicated that, compared to the CU Aβ− group, the magnitude of Ch4p volume loss was significantly greater in the CU Aβ+ and CI Aβ+ (Cohen's d = 0.90 and 1.89) groups, but not in the CI Aβ− group (Cohen's d = 0.15, p = 0.423). The CI Aβ+ group showed a greater rate of Ch4p volume loss (Cohen's d = 0.92) compared to the CU Aβ+ group. The trajectories of Ch4p volume loss in different groups are illustrated in Fig. 3A.

For Ch1/Ch2, the group × time interaction from LMM was significant (F = 31.89, p < 0.001). The CU Aβ− group showed a rate of Ch1/Ch2 volume loss of −0.033 ± 0.006 SD per year (∼−0.31%/y), while the CU Aβ+ and CI Aβ+ groups exhibited a greater average rate of −1.32 and −1.47%/y. The interaction contrasts between groups indicated that, compared to the CU Aβ− group, the magnitude of Ch1/Ch2 volume loss was significantly greater in the CU Aβ+, CI Aβ+, and CI Aβ− groups (all Cohen's d > 0.8, Table 2). Comparing the CU Aβ+ and CI Aβ+ groups revealed no significant difference in the rate of Ch1/Ch2 volume loss (Cohen's d = 0.12). The trajectories of Ch1/Ch2 volume loss in different groups are shown in Fig. 3B.

Fig. 4 compares the effect sizes of AD-related group contrasts between the BF and hippocampus as well as within the BF subregions. All 4 ROIs yielded comparable effect sizes in the comparisons with the CU Aβ− group, with large effect sizes between CU Aβ− and CU Aβ+ groups and much greater effect sizes (all Cohen's d > 1.5) between CU Aβ− and CI Aβ+ groups. Comparing between the CU Aβ+ and CI Aβ+ groups yielded the largest effect size of differences in the rate of volume loss in the Ch4p region, while no significant differences with a small effect size were noted in the Ch1/Ch2 region.

Moreover, Fig. 5 shows negative associations between Aβ levels at baseline and the rates of volume loss for the entire BF and hippocampus as well as for the BF subregions. Among CU individuals,

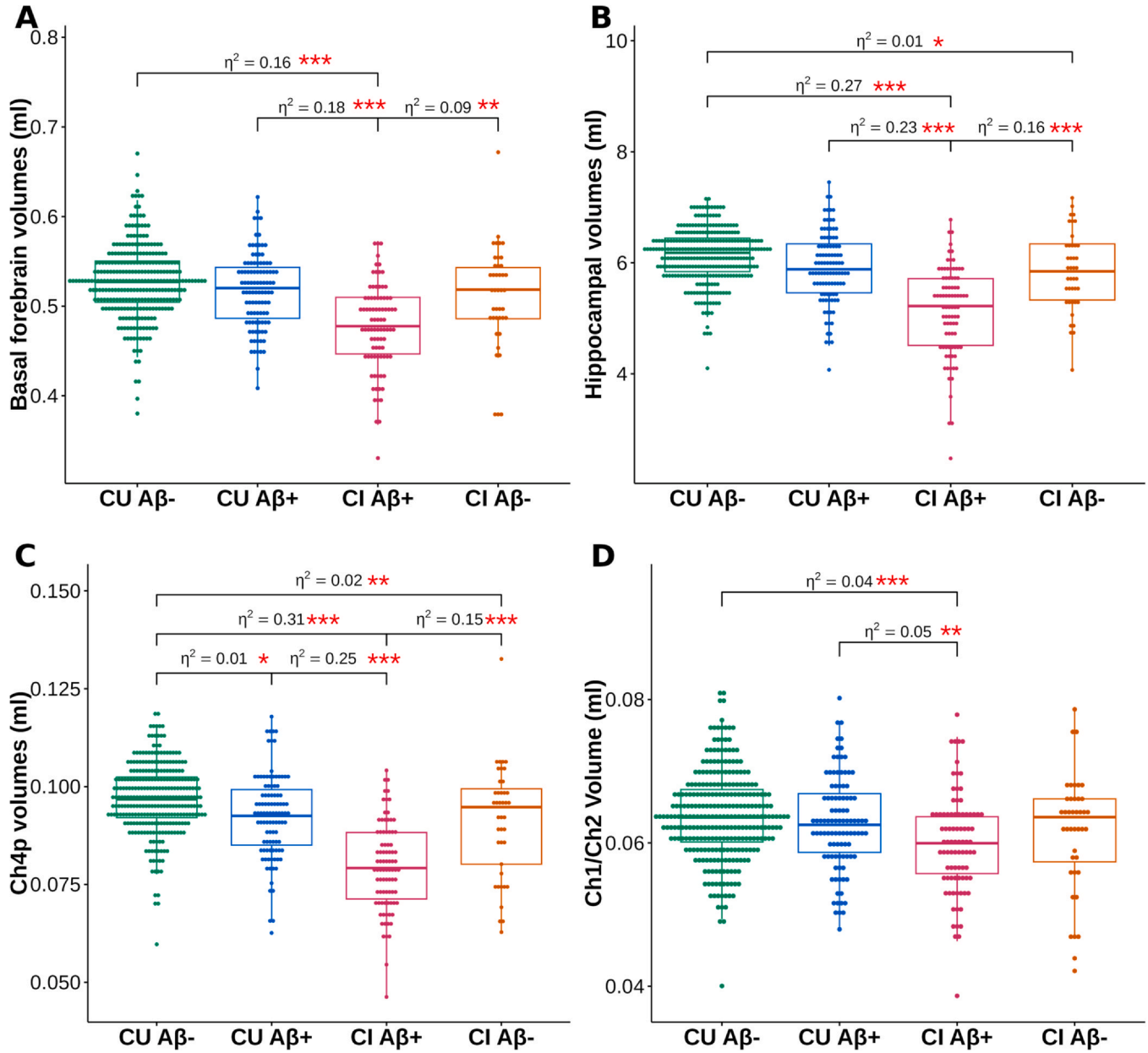

Fig. 1. Boxplots of volumetric measures at baseline of (A) total basal forebrain, (B) hippocampus, (C) Ch4p, and (D) Ch1/Ch2 for the 4 classification groups. All the volumetric measures were adjusted for multiscanner effects and the effect of total intracranial volumes. The η^2 values indicate the effect sizes of pairwise group differences, adjusting for age, sex, and education. The significance of the difference after correcting for multiple comparisons was indicated (in red) as $^*p < 0.5$, $^{**}p < 0.01$, $^{***}p < 0.001$. Abbreviations: Aβ, amyloid-beta; Ch1/Ch2, the medial septal nucleus and vertical limb of the diagonal band of Broca; Ch4p, the posterior subdivision of the nucleus basalis of Meynert; CI, cognitively impaired; CU, cognitively unimpaired.

higher Aβ levels at baseline were associated with greater rates of volume loss in the total BF, hippocampus, and BF subregions, with moderate effect sizes (all Pearson's R between −0.39 and −0.49). When investigating among CI individuals, compared to the Ch1/Ch2 subregion, stronger associations were observed for Ch4p and hippocampus (R = −0.65 and −0.59).

4. Discussion

This study showed the nature and magnitude of volume loss in the BF and its subregions over periods of up to 14 years during aging (i.e., CU Aβ−) and through the preclinical (i.e., CU Aβ+) and symptomatic (i.e., CI Aβ+) stages of AD. First, this study provides reliable estimates of changes in BFV and HV during normal aging over the longest periods studied to date (14 years). Moreover, the cohort studied in this work represents an excellent basis for understanding the effect of early AD on the predominantly cholinergic BF region as, by design, participants recruited in the AIBL study have a very low prevalence of uncontrolled or severe cardiovascular disease and frank cerebrovascular disease (Ellis et al., 2009; Harrington et al., 2017). All AIBL individuals also undergo regular PET and MRI scans for assessing Aβ burden and brain atrophy as well as health and

Table 2
Linear mixed-effects models examining the rates of volume loss between groups for the total BF, hippocampus, and the BF subregions

Brain region	Contrast	Estimate[a] (Std. error)	*p*-value[b]	Cohen's *d*
Total BF	CU Aβ− versus CU Aβ+	−0.161 (0.022)	< 0.001	1.20
	CU Aβ− versus CI Aβ+	−0.185 (0.028)	< 0.001	1.53
	CU Aβ− versus CI Aβ−	−0.065 (0.031)	0.009	0.51
	CU Aβ+ versus CI Aβ+	−0.024 (0.032)	0.266	0.18
Hippocampus	CU Aβ− versus CU Aβ+	−0.143 (0.016)	< 0.001	1.02
	CU Aβ− versus CI Aβ+	−0.249 (0.019)	< 0.001	1.85
	CU Aβ− versus CI Aβ−	−0.027 (0.022)	0.398	0.21
	CU Aβ+ versus CI Aβ+	−0.106 (0.022)	< 0.001	0.61
Ch4p	CU Aβ− versus CU Aβ+	−0.081 (0.013)	< 0.001	0.90
	CU Aβ− versus CI Aβ+	−0.162 (0.017)	< 0.001	1.89
	CU Aβ− versus CI Aβ−	−0.013 (0.018)	0.423	0.15
	CU Aβ+ versus CI Aβ+	−0.082 (0.019)	< 0.001	0.92
Ch1/Ch2	CU Aβ− versus CU Aβ+	−0.102 (0.013)	< 0.001	1.32
	CU Aβ− versus CI Aβ+	−0.111 (0.017)	< 0.001	1.53
	CU Aβ− versus CI Aβ−	−0.060 (0.018)	< 0.001	0.80
	CU Aβ+ versus CI Aβ+	−0.009 (0.019)	0.423	0.12

Key: Aβ, amyloid-beta; BF, basal forebrain; Ch1/Ch2, the medial septal nucleus and vertical limb of the diagonal band of Broca; Ch4p, the posterior subdivision of the nucleus basalis of Meynert; CI, cognitively impaired; CU, cognitively unimpaired.
[a] Standardized coefficients were estimated from linear mixed-effect models using standardized scores of volumetric data.
[b] All *p* values were corrected for multiple comparisons.

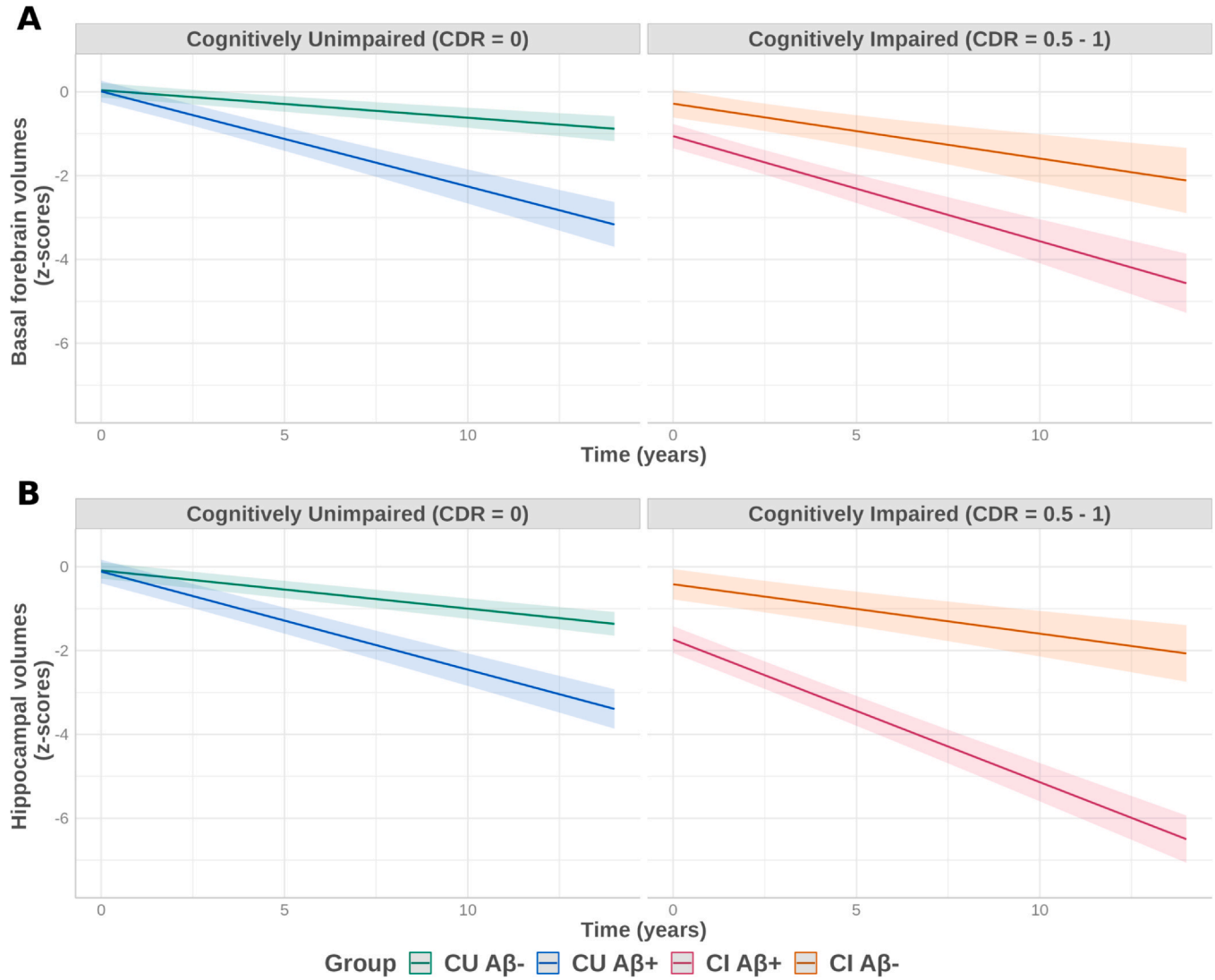

Fig. 2. Volume trajectories by group for the (A) total basal forebrain and (B) hippocampus. Shaded regions show 95% confidence intervals. The y-axis was normalized using the mean and standard deviation of the baseline volumetric measures in the CU Aβ− group. Abbreviations: Aβ, amyloid-beta; CDR, clinical dementia rating; CI, cognitively impaired; CU, cognitively unimpaired.

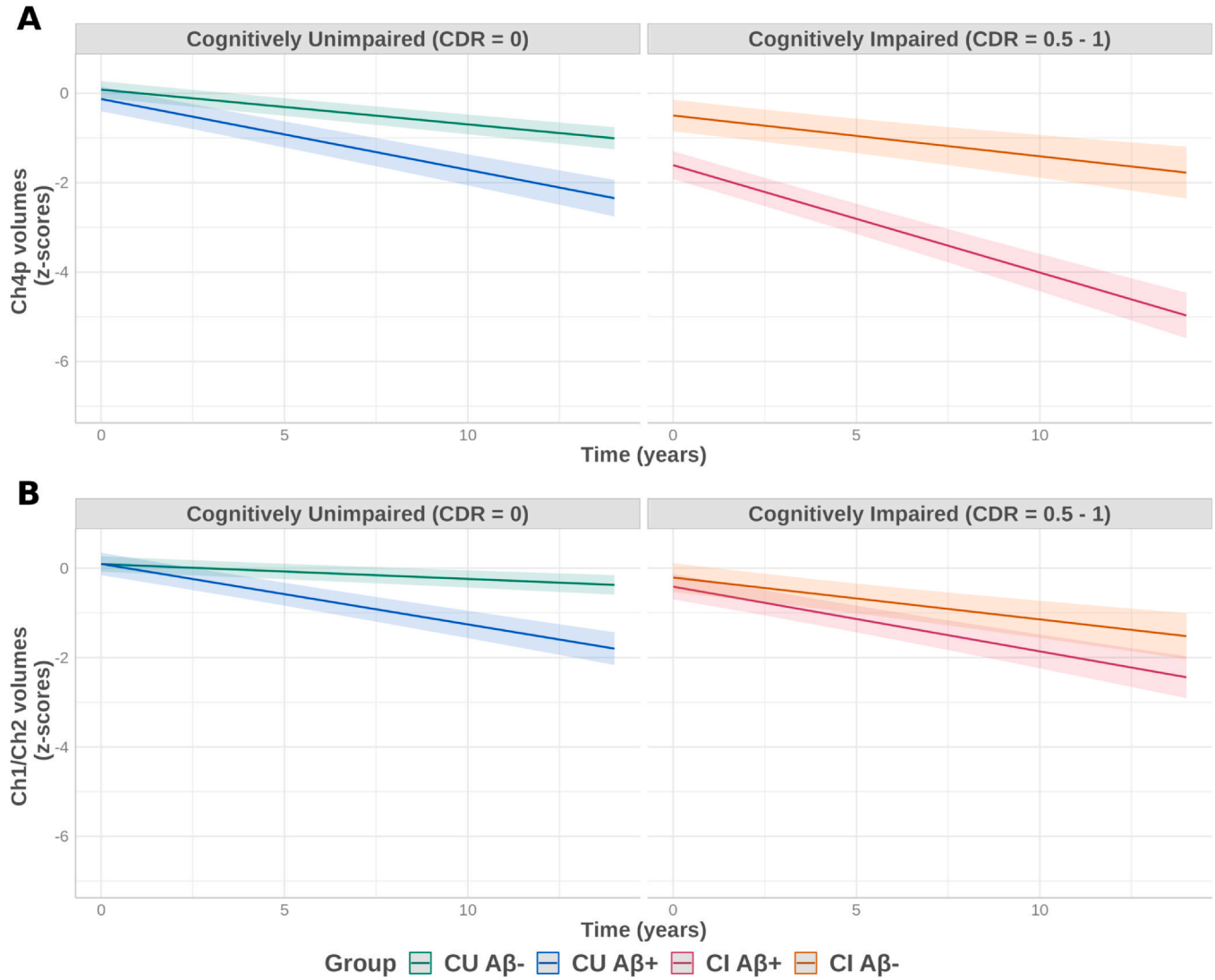

Fig. 3. Subregional BF volume trajectories by group for the (A) Ch4p and (B) Ch1/Ch2. Shaded regions show 95% confidence intervals. The y-axis was normalized using the mean and standard deviation of the baseline volumetric measures in the CU Aβ− group. Abbreviations: Aβ, amyloid-beta; Ch1/Ch2, the medial septal nucleus and vertical limb of the diagonal band of Broca; Ch4p, the posterior subdivision of the nucleus basalis of Meynert; CDR, clinical dementia rating; CI, cognitively impaired; CU, cognitively unimpaired.

clinical disease status evaluations every 18 months. Therefore, volumetric changes in CU Aβ− individuals provide a robust estimate of age-related change in the BF and hippocampus and serve as a strong reference point for understanding any disease-related changes in these regions.

When compared to CU Aβ− adults cross sectionally, adults with mild symptomatic disease (i.e., CDR = 0.5 and 1) had substantially smaller total BFV and HV. This brain volume reduction is consistent with that observed previously in adults with AD dementia using older clinical classification systems, as well as with newer criteria with positive AD biomarkers (Grothe et al., 2012; Kerbler et al., 2015; Teipel et al., 2014). However, the measurement of BFV and HV showed limited utility in differentiating early symptomatic and preclinical AD as measures of these regions in the CU Aβ+ group remained within normal limits (Fig. 1). When considered in terms of the BF subregions, our analyses showed that BFV loss was nonuniform, consistent with the heterogeneous distribution of BF cholinergic cells and their differential vulnerability to AD pathology (Schmitz and Zaborszky, 2021; Teipel et al., 2005). For example, the magnitude of volume reduction in the predominantly cholinergic subregion of Ch4p was greater than that observed in the Ch1/Ch2 region in both Aβ+ groups, with Ch4p volume reduced to a greater magnitude in the CI Aβ+ group (Fig. 1C). These findings are consistent with the substantial bilateral volume reduction of the nucleus basalis Meynert (Ch4) observed in preclinical AD (Cantero et al., 2020). Overall, these data indicate that the BFV reduction in both presymptomatic and early symptomatic AD is greatest in Ch4p, which is known to provide cholinergic innervation to AD-vulnerable brain regions (e.g., the superior temporal and temporal pole) (Liu et al., 2015; Mesulam et al., 1983), with the magnitude of this volume reduction greater than that observed for HV. Thus, single-time-point MRI examinations aiming to identify AD in individuals at risk of the disease could be strengthened by focusing on Ch4p volumes.

The relationship between AD biomarkers and clinical symptoms on BFV becomes most apparent from consideration of BFV changes longitudinally. Considered in terms of the total volume, mild BFV loss occurs as part of normal aging, with an average rate of −0.50% per year in CU Aβ− adults. Compared to these adults, volume loss in the BF was increased substantially with abnormal

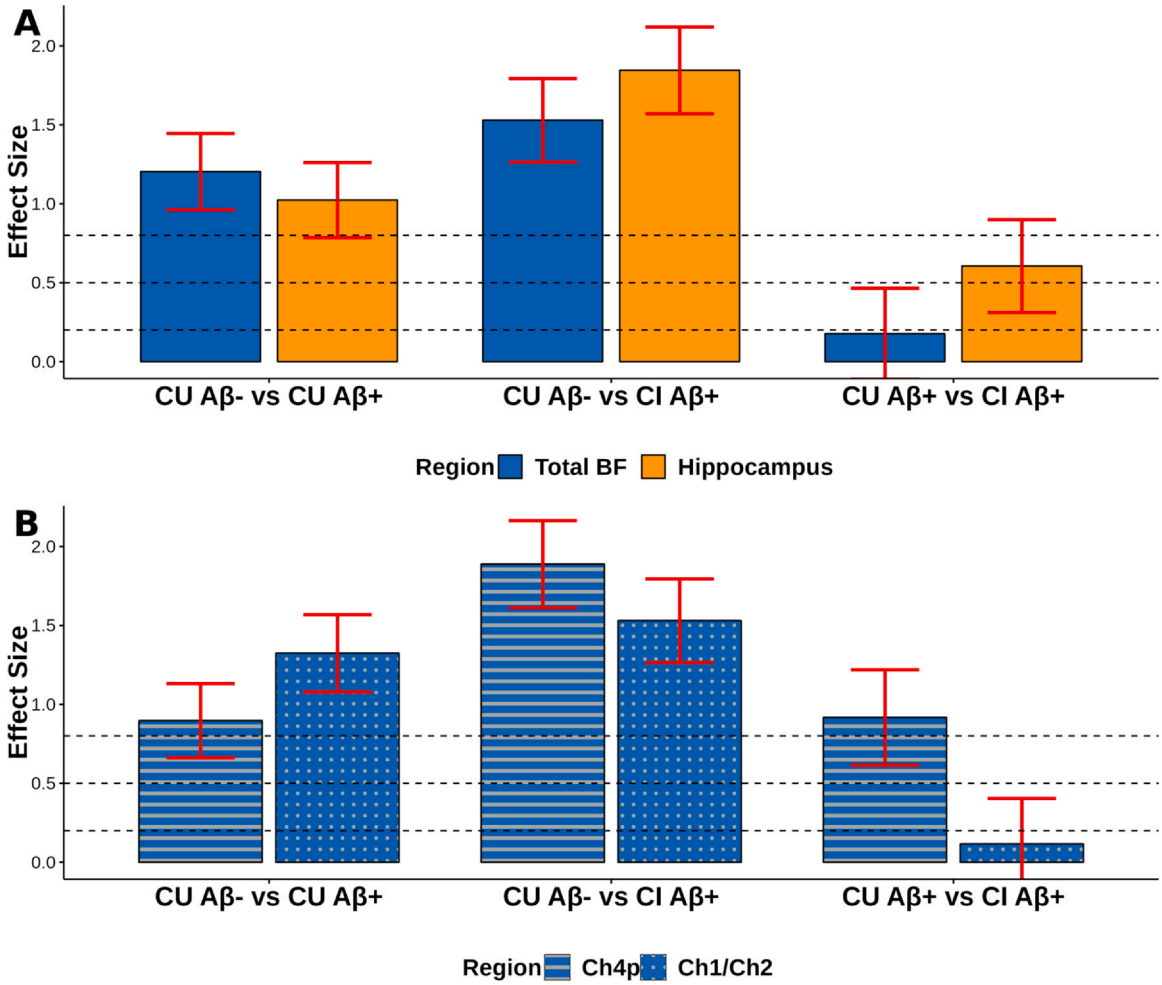

Fig. 4. Effect sizes (Cohen's *d*) of pairwise group contrasts for the rates of volume loss that were compared (A) between the total BF and hippocampus as well as (B) between Ch4p and Ch1/Ch2. The dashed lines indicate the cut-off values of $d = 0.2$, 0.6, and 0.8 for the small, medium, and large effect sizes. The 95% confidence intervals associated with each effect size (i.e., error bars in red) were estimated using a bootstrap procedure with 1000 replications. Abbreviations: Aβ, amyloid-beta; BF, basal forebrain; Ch1/Ch2, the medial septal nucleus and vertical limb of the diagonal band of Broca; Ch4p, the posterior subdivision of the nucleus basalis of Meynert; CI, cognitively impaired; CU, cognitively unimpaired.

Aβ levels, even in the absence of any cognitive impairment (CU Aβ+), showing average annual rates of −1.75 and −2.12%/y. These are comparable with the former investigation that showed annual rates of −1.6% and −2.9% among healthy elderly and patients with very mild AD who experienced disease progression (Grothe et al., 2013). Although a similar pattern of decline was observed for HV in CU individuals, Aβ-dependent HV loss was much greater (e.g., almost double) for individuals with mild symptomatic disease (Fig. 2B). However, in the absence of abnormal Aβ levels, age-related HV loss was not influenced by the presence of mild dementia symptoms. Together, they suggest that progressive AD-related dementia symptoms including memory loss most likely reflect the loss of both cholinergic neurons in the BF and neurons in the hippocampus.

Reconsideration of the effect of Aβ levels on volume loss over time within the BF subregions confirmed the early and selective vulnerability of the Ch4p region to progression of AD pathology (Cantero et al., 2020; Teipel et al., 2014). The cholinergic neuron-rich Ch4p area first started with more age-related volume loss (−0.72%/y, −0.61%/y within 5 years, Supplementary Table 2), which was double that observed for Ch1/Ch2 (−0.31%/y, −0.42%/y within 5 years). This age-related decline in BF subregions was increased by the presence of abnormal Aβ levels, although this increase was much greater for the Ch4p subregion in those with mild symptomatic disease (−2.74%/y, −2.85%/y within 5 years, Fig. 3). In adults with clinical symptoms but no abnormal Aβ levels, the rate of volume loss was increased slightly in Ch1/Ch2 but not in Ch4p (Fig. 3).

Through the combination of cross-sectional and longitudinal analyses, in large well-described clinical groups, studied over extended periods, this study provides an improved understanding of the involvement of the BF, and BF subregions (Ch4p and Ch1/Ch2), in normal aging, preclinical, and symptomatic AD. These findings demonstrate that reduced Ch4p volumes can be detected cross sectionally in preclinical AD, and that there is a rapid volume loss in this area associated with abnormal Aβ levels. While little Ch1/Ch2 volume reduction was observed cross sectionally, the rate of volume loss in Ch1/Ch2 was also increased, to a large extent, by abnormal Aβ levels, at the preclinical stage. However, this Aβ-related volume loss remained unaffected by the presence of mild dementia symptoms (i.e., CI Aβ+). Furthermore, the post-hoc analyses demonstrate clearly that higher Aβ levels are associated with faster volume loss to the same extent for both subregions among CU individuals; however, in older individuals with cognitive impairment, this association was weakened in the Ch1/Ch2 subregion (Fig. 5).

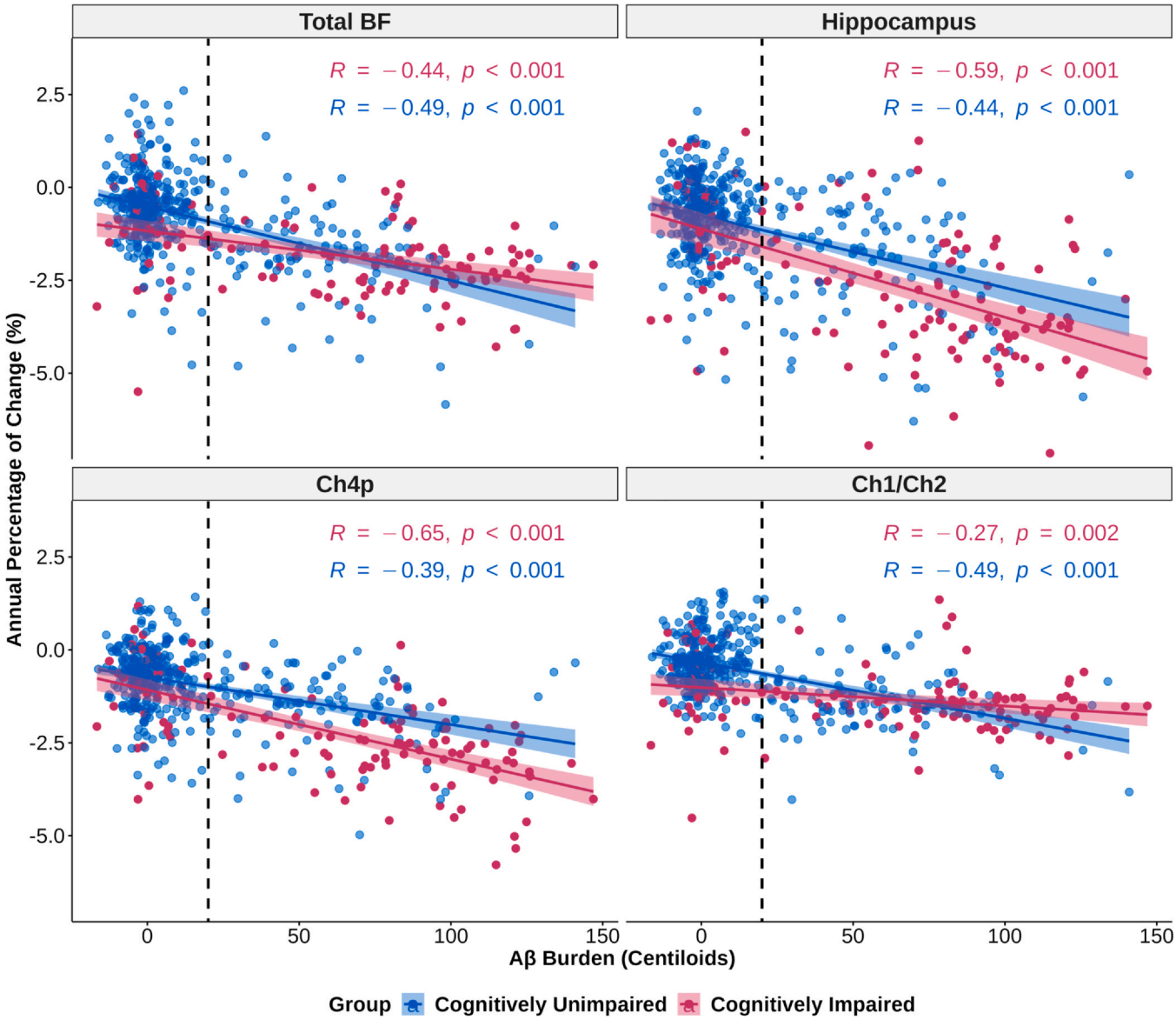

Fig. 5. Correlation analysis of Aβ burden at baseline and the rate of volume loss (in %/y) for the total BF, hippocampus, Ch4p, and Ch1/Ch2 among cognitively unimpaired (blue) and cognitively impaired (red) individuals. Abbreviations: Aβ, amyloid-beta; BF, basal forebrain; Ch1/Ch2, the medial septal nucleus and vertical limb of the diagonal band of Broca; Ch4p, the posterior subdivision of the nucleus basalis of Meynert.

Overall, this study represents an advancement in the continued efforts to delineate the longitudinal changes of volume in the global and subregional BF across the AD spectrum. First, the data presented here were derived from a large carefully-assessed cohort of older adults with longitudinal MRI data over an average period of 5 years as well as the use of PET to measure Aβ levels. Secondly, while the early involvement of the Ch4p subregion in the preclinical AD has been well-established (Cantero et al., 2020; Grothe et al., 2012), the findings presented here further clarify the involvement of the Ch1/Ch2 subregion, containing the second largest cholinergic cell group in the BF, in the course of AD. It is known that cholinergic cells in these 2 subregions project to different brain regions within different functional networks, where Ch4p provides cholinergic innervation to temporal pole and superior temporal and Ch1/Ch2 innervates the hippocampus (Liu et al., 2015; Schmitz and Zaborszky, 2021). Distinguishing differences in volume loss trajectories between Ch4p and Ch1/Ch2 subregions would be beneficial for understanding and differentiating their roles involved in different cognitive deficits in early symptomatic and preclinical AD. Future explorations into the correlations between subregional BF atrophy and the decline across different cognitive domains may enhance our understanding of the neural basis underpinning the heterogeneity of cognitive decline in early AD.

Some caveats do operate to limit the generalizability of current findings. First, in the current cohort, we have not considered the levels of tau pathology in the grouping strategy due to the limited availability of cerebrospinal fluid and PET data at baseline (and earlier visits) in the AIBL study. Recent studies suggest the correlation of tau pathology with BFV loss in individuals at risk for AD (Cantero et al., 2020; Cavedo et al., 2020). It is most likely that the observed link between BFV loss and Aβ pathology could be (directly or partially) mediated by the levels of tau. However, this study seeks mainly to determine the nature and rate of volume loss in the BF, and future studies will be conducted to understand the neurobiological basis of this change with the emerging data (e.g., PET and plasma biomarkers) for tau pathology. Second, it is important to be

aware that volumetric measures used in this work quantify gross tissue changes rather than the cholinergic neuron degeneration in the BF. Our results are to some extent inconclusive with respect to the longitudinal neuron loss in the cholinergic BF system. Nevertheless, the posterior BF nuclei have a high proportion (~80%) of cholinergic neurons compared to the more heterogeneous anterior Ch1/Ch2 nuclei (Zaborszky et al., 2008), which likely impacts the degree of volume loss relative to the cholinergic neuronal loss. Lastly, AIBL participants were volunteers who were not randomly selected from the community, were generally well educated, and had high scores on cognitive tests and a low prevalence of comorbidities. These findings thus might only be valid in similar cohorts, and this limitation precludes the generalization of the findings to the general population. Future work incorporating molecular imaging biomarkers for specific assessment of the cholinergic cell groups would be beneficial to confirm our findings (Craig et al., 2020; Xia et al., 2022).

In conclusion, the current data provide further understanding of the nature and magnitude of volume loss in the BF as well as the subregions across different stages of AD. These findings strongly support the early and substantial vulnerability of the BF and further reveal the distinctive degeneration of BF subregions in normal aging and AD. As the preclinical stages of AD could span more than a decade and are beyond the reach of current clinical treatment, consideration of BF cholinergic degeneration could provide further insight into AD pathophysiology before the emergence of cognitive symptoms and might potentially facilitate the development of interventions aimed at protecting the vulnerabilities of BF cholinergic neurons in the preclinical window of AD.

Verification.

We confirm that this work is original and has not been published elsewhere, nor is it currently under consideration for publication elsewhere. We will not submit this manuscript elsewhere while it is under consideration at the Neurobiology of Aging. Approval for the Australian Imaging, Biomarkers and Lifestyle study was obtained from the institutional ethics committees of Austin Health, St Vincent's Health, Hollywood Private Hospital, and Edith Cowan University. Written informed consent was obtained from all volunteers before participation. I confirm that all authors have reviewed the contents of the manuscript, approve of its contents, and validate the accuracy of the data.

Funding

The Australian Imaging, Biomarkers and Lifestyle study (http://www.AIBL.csiro.au) is a consortium between Austin Health, CSIRO, Edith Cowan University, the Florey Institute (The University of Melbourne), and the National Ageing Research Institute. Partial financial support provided by the Alzheimer's Association (US), the Alzheimer's Drug Discovery Foundation, an anonymous foundation, the Science and Industry Endowment Fund, the Dementia Collaborative Research Centres, the Victorian Government's Operational Infrastructure Support program, the McCusker Alzheimer's Research Foundation, the National Health and Medical Research Council, as well as the Cooperative Research Centre for Mental Health. Numerous commercial interactions have supported data collection and analysis. In-kind support has also been provided by Sir Charles Gairdner Hospital, the University of Melbourne, and St Vincent's Hospital.

CRediT authorship contribution statement

Ying Xia: Conceptualization, Software, Formal analysis, Data curation, Writing – original draft, review & editing. **Paul Maruff**: Conceptualization, Methodology, Formal analysis, Supervision, Writing – review & editing. **Vincent Doré**: Data curation, Supervision, Writing – review & editing. **Pierrick Bourgeat**: Software, Data curation, Writing – review & editing. **Simon M. Laws**: Data curation, Writing – review & editing. **Christopher Fowler**: Resources, Investigation. **Stephanie R. Rainey-Smith**: Resources, Writing – review & editing. **Ralph N. Martins**: Resources, Writing – review & editing. **Victor L. Villemagne**: Resources, Writing – review & editing. **Christopher C. Rowe**: Resources, Writing – review & editing. **Colin L. Masters**: Resources, Writing – review & editing. **Elizabeth J. Coulson**: Conceptualization, Supervision, Writing – review & editing. **Jurgen Fripp**: Conceptualization, Supervision, Writing – review & editing.

Disclosure statement

All authors report no conflicts of interest relevant to this article.

Acknowledgements

We thank all those who took part as subjects in the study for their commitment and dedication to helping advance research into the early detection and causation of AD. We kindly thank all Australian Imaging, Biomarkers and Lifestyle (AIBL) Research Group members (http://aibl.csiro.au/about/aibl-research-team/). The AIBL study (http://www.AIBL.csiro.au) is a consortium between Austin Health, CSIRO, Edith Cowan University, the Florey Institute (The University of Melbourne), and the National Ageing Research Institute. Partial financial support provided by the Alzheimer's Association (US), the Alzheimer's Drug Discovery Foundation, an Anonymous foundation, the Science and Industry Endowment Fund, the Dementia Collaborative Research Centres, the Victorian Government's Operational Infrastructure Support program, the McCusker Alzheimer's Research Foundation, the National Health and Medical Research Council, as well as the Cooperative Research Centre for Mental Health. Numerous commercial interactions have supported data collection and analysis. In-kind support has also been provided by Sir Charles Gairdner Hospital, the University of Melbourne, and St Vincent's Hospital.

Supplementary material

Supplementary material associated with this article can be found in the online version at doi:10.1016/j.neurobiolaging.2023.09.002.

References

Ashburner, J., 2007. A fast diffeomorphic image registration algorithm. Neuroimage 38 (1), 95–113. https://doi.org/10.1016/j.neuroimage.2007.07.007

Ballinger, E.C., Ananth, M., Talmage, D.A., Role, L.W., 2016. Basal forebrain cholinergic circuits and signaling in cognition and cognitive decline. Neuron 91 (6), 1199–1218. https://doi.org/10.1016/j.neuron.2016.09.006

Beer, J.C., Tustison, N.J., Cook, P.A., Davatzikos, C., Sheline, Y.I., Shinohara, R.T., Linn, K.A., 2020. Longitudinal ComBat: a method for harmonizing longitudinal multi-scanner imaging data. Neuroimage 220, 117129. https://doi.org/10.1016/j.neuroimage.2020.117129

Bohnen, N.I., Grothe, M.J., Ray, N.J., Müller, M.L.T.M., Teipel, S.J., 2018. Recent advances in cholinergic imaging and cognitive decline—revisiting the cholinergic hypothesis of dementia. Curr. Geriatr. Rep. 7 (1), 1–11. https://doi.org/10.1007/s13670-018-0234-4

Bourgeat, P., Doré, V., Doecke, J., Ames, D., Masters, C.L., Rowe, C.C., Fripp, J., Villemagne, V.L., 2021. Non-negative matrix factorisation improves Centiloid robustness in longitudinal studies. Neuroimage 226, 117593. https://doi.org/10.1016/j.neuroimage.2020.117593

Bourgeat, P., Villemagne, V.L., Dore, V., Brown, B., Macaulay, S.L., Martins, R., Masters, C.L., Ames, D., Ellis, K., Rowe, C.C., Salvado, O., Fripp, J., 2015. Comparison of MR-less PiB SUVR quantification methods. Neurobiol. Aging 36, S159–S166. https://doi.org/10.1016/j.neurobiolaging.2014.04.033

Brauer, K., Schober, A., Wolff, J.R., Winkelmann, E., Luppa, H., Lüth, H.J., Böttcher, H., 1991. Morphology of neurons in the rat basal forebrain nuclei: comparison between NADPH-diaphorase histochemistry and immunohistochemistry of glutamic acid decarboxylase, choline acetyltransferase, somatostatin and parvalbumin. J. Hirnforsch. 32 (1), 1–17.

Cantero, J.L., Atienza, M., Lage, C., Zaborszky, L., Vilaplana, E., Lopez-Garcia, S., Pozueta, A., Rodriguez-Rodriguez, E., Blesa, R., Alcolea, D., Lleo, A., Sanchez-Juan, P., Fortea, J., Alzheimer's Disease Neuroimaging I, 2020. Atrophy of basal forebrain initiates with tau pathology in individuals at risk for Alzheimer's disease. Cereb. Cortex 30 (4), 2083–2098. https://doi.org/10.1093/cercor/bhz224

Cantero, J.L., Zaborszky, L., Atienza, M., 2017. Volume loss of the nucleus basalis of meynert is associated with atrophy of innervated regions in mild cognitive impairment. Cereb. Cortex 27 (8), 3881–3889. https://doi.org/10.1093/cercor/bhw195

Cavedo, E., Lista, S., Houot, M., Vergallo, A., Grothe, M.J., Teipel, S., Zetterberg, H., Blennow, K., Habert, M.-O., Potier, M.C., Dubois, B., Hampel, H., for the I-pSG, the Alzheimer Precision Medicine I, 2020. Plasma tau correlates with basal forebrain atrophy rates in people at risk for Alzheimer disease. Neurology 94 (1), e30. https://doi.org/10.1212/WNL.0000000000008696

Clark, C.M., Schneider, J.A., Bedell, B.J., Beach, T.G., Bilker, W.B., Mintun, M.A., Av45-A07 Study Group ft, 2011. Use of florbetapir-PET for imaging β-amyloid pathology. JAMA 305 (3), 275–283. https://doi.org/10.1001/jama.2010.2008

Cohen, J., 1973. Eta-squared and partial eta-squared in fixed factor ANOVA designs. Educ. Psychol. Meas. 33 (1), 107–112.

Craig, C.E., Ray, N.J., Müller, M., Bohnen, N.I., 2020. New developments in cholinergic imaging in Alzheimer and Lewy body disorders. Curr. Behav. Neurosci. Rep. 7 (4), 278–286. https://doi.org/10.1007/s40473-020-00221-6

Doré, V., Bullich, S., Rowe, C.C., Bourgeat, P., Konate, S., Sabri, O., Stephens, A.W., Barthel, H., Fripp, J., Masters, C.L., Dinkelborg, L., Salvado, O., Villemagne, V.L., De Santi, S., 2019. Comparison of 18F-florbetaben quantification results using the standard Centiloid, MR-based, and MR-less CapAIBL® approaches: validation against histopathology. Alzheimers Dement. 15 (6), 807–816. https://doi.org/10.1016/j.jalz.2019.02.005

Ellis, K.A., Bush, A.I., Darby, D., De Fazio, D., Foster, J., Hudson, P., Ames, D., 2009. The Australian Imaging, Biomarkers and Lifestyle (AIBL) study of aging: methodology and baseline characteristics of 1112 individuals recruited for a longitudinal study of Alzheimer's disease. Int. Psychogeriatr. 21 (4), 672–687. https://doi.org/10.1017/S1041610209009405

Fowler, C., Rainey-Smith, S.R., Bird, S., Bomke, J., Bourgeat, P., Brown, B.M., Burnham, S.C., Bush, A.I., Chadunow, C., Collins, S., Doecke, J., 2021. Fifteen years of the Australian Imaging, Biomarkers and Lifestyle (AIBL) study: progress and observations from 2,359 older adults spanning the spectrum from cognitive normality to Alzheimer's disease. J. Alzheimers Dis. Rep. 5, 443–468. https://doi.org/10.3233/ADR-210005

Francis, P.T., Palmer, A.M., Snape, M., Wilcock, G.K., 1999. The cholinergic hypothesis of Alzheimer's disease: a review of progress. J. Neurol. Neurosurg. Psychiatry 66 (2), 137. https://doi.org/10.1136/jnnp.66.2.137

Gaser, C., Dahnke, R., Thompson, P.M., Kurth, F., Luders, E., 2022. CAT – a computational anatomy toolbox for the analysis of structural MRI data. bioRxiv. doi: 10.1101/2022.06.11.495736.

Geula, C., Dunlop, S.R., Ayala, I., Kawles, A.S., Flanagan, M.E., Gefen, T., Mesulam, M.-M., 2021. Basal forebrain cholinergic system in the dementias: vulnerability, resilience, and resistance. J. Neurochem. 158 (6), 1394–1411. https://doi.org/10.1111/jnc.15471

Grothe, M., Heinsen, H., Teipel, S., 2013. Longitudinal measures of cholinergic forebrain atrophy in the transition from healthy aging to Alzheimer's disease. Neurobiol. Aging 34 (4), 1210–1220. https://doi.org/10.1016/j.neurobiolaging.2012.10.018

Grothe, M., Heinsen, H., Teipel, S.J., 2012. Atrophy of the cholinergic basal forebrain over the adult age range and in early stages of Alzheimer's disease. Biol. Psychiatry 71 (9), 805–813. https://doi.org/10.1016/j.biopsych.2011.06.019

Grothe, M.J., Ewers, M., Krause, B., Heinsen, H., Teipel, S.J., 2014. Basal forebrain atrophy and cortical amyloid deposition in nondemented elderly subjects. Alzheimers Dement. 10 (5S), S344–S353. https://doi.org/10.1016/j.jalz.2013.09.011

Hampel, H., Mesulam, M.M., Cuello, A.C., Farlow, M.R., Giacobini, E., Grossberg, G.T., Khachaturian, A.S., Vergallo, A., Cavedo, E., Snyder, P.J., Khachaturian, Z.S., 2018. The cholinergic system in the pathophysiology and treatment of Alzheimer's disease. Brain 141 (7), 1917–1933. https://doi.org/10.1093/brain/awy132

Harrington, K.D., Lim, Y.Y., Ames, D., Hassenstab, J., Rainey-Smith, S., Robertson, J., Salvado, O., Masters, C.L., Maruff, P., for the ARG, 2017. Using robust normative data to investigate the neuropsychology of cognitive aging. Arch. Clin. Neuropsychol. 32 (2), 142–154. https://doi.org/10.1093/arclin/acw106

Kerbler, G.M., Fripp, J., Rowe, C.C., Villemagne, V.L., Salvado, O., Rose, S., Coulson, E.J., 2015. Basal forebrain atrophy correlates with amyloid β burden in Alzheimer's disease. NeuroImage Clin. 7, 105–113. https://doi.org/10.1016/j.nicl.2014.11.015

Kilimann, I., Grothe, M., Heinsen, H., Alho, E.J.L., Grinberg, L., Amaro Jr, E., dos Santos, G.A.B., da Silva, R.E., Mitchell, A.J., Frisoni, G.B., Bokde, A.L.W., Fellgiebel, A., Filippi, M., Hampel, H., Klöppel, S., Teipel, S.J., 2014. Subregional basal forebrain atrophy in Alzheimer's disease: a multicenter study. J. Alzheimers Dis. 40, 687–700. https://doi.org/10.3233/JAD-132345

Liu, A.K., Chang, R.C., Pearce, R.K., Gentleman, S.M., 2015. Nucleus basalis of Meynert revisited: anatomy, history and differential involvement in Alzheimer's and Parkinson's disease. Acta Neuropathol. 129 (4), 527–540. https://doi.org/10.1007/s00401-015-1392-5

McKhann, G., Drachman, D., Folstein, M., Katzman, R., Price, D., Stadlan, E.M., 1984. Clinical diagnosis of Alzheimer's disease. Neurology 34 (7), 939. https://doi.org/10.1212/WNL.34.7.939

Mesulam, M.M., 1998. From sensation to cognition. Brain 121 (6), 1013–1052. https://doi.org/10.1093/brain/121.6.1013

Mesulam, M.M., Mufson, E.J., Levey, A.I., Wainer, B.H., 1983. Cholinergic innervation of cortex by the basal forebrain: cytochemistry and cortical connections of the septal area, diagonal band nuclei, nucleus basalis (Substantia innominata), and hypothalamus in the rhesus monkey. J. Comp. Neurol. 214 (2), 170–197. https://doi.org/10.1002/cne.902140206

Morris, J.C., 1993. The Clinical Dementia Rating (CDR): current version and scoring rules. Neurology 43, 2412–2414. https://doi.org/10.1212/WNL.43.11.2412-a

Müller, P., Vellage, A.-K., Schmicker, M., Menze, I., Grothe, M.J., Teipel, S.J., Müller, N.G., 2021. Structural MRI of the basal forebrain as predictor of cognitive response to galantamine in healthy older adults—a randomized controlled double-blinded crossover study. Alzheimers Dement. Transl. Res. Clin. Interv. 7 (1), e12153. https://doi.org/10.1002/trc2.12153

Petersen, R.C., Smith, G.E., Waring, S.C., Ivnik, R.J., Tangalos, E.G., Kokmen, E., 1999. Mild cognitive impairment: clinical characterization and outcome. Arch. Neurol. 56 (3), 303–308. https://doi.org/10.1001/archneur.56.3.303

Prado, V.F., Janickova, H., Al-Onaizi, M.A., Prado, M.A.M., 2017. Cholinergic circuits in cognitive flexibility. Neuroscience 345, 130–141. https://doi.org/10.1016/j.neuroscience.2016.09.013

Ramos-Rodriguez, J.J., Pacheco-Herrero, M., Thyssen, D., Murillo-Carretero, M.I., Berrocoso, E., Spires-Jones, T.L., Bacskai, B.J., Garcia-Alloza, M., 2013. Rapid β-amyloid deposition and cognitive impairment after cholinergic denervation in APP/PS1 mice. J. Neuropathol. Exp. Neurol. 72 (4), 272–285. https://doi.org/10.1097/NEN.0b013e318288a8dd

Rowe, C.C., Ellis, K.A., Rimajova, M., Bourgeat, P., Pike, K.E., Jones, G., Villemagne, V.L., 2010. Amyloid imaging results from the Australian Imaging, Biomarkers and Lifestyle (AIBL) study of aging. Neurobiol. Aging 31 (8), 1275–1283. https://doi.org/10.1016/j.neurobiolaging.2010.04.007

Scheef, L., Grothe, M.J., Koppara, A., Daamen, M., Boecker, H., Biersack, H., Schild, H.H., Wagner, M., Teipel, S., Jessen, F., 2019. Subregional volume reduction of the cholinergic forebrain in subjective cognitive decline (SCD). NeuroImage Clin. 21, 101612. https://doi.org/10.1016/j.nicl.2018.101612

Schliebs, R., 2005. Basal forebrain cholinergic dysfunction in Alzheimer's disease – interrelationship with β-amyloid, inflammation and neurotrophin signaling. Neurochem. Res. 30 (6), 895–908. https://doi.org/10.1007/s11064-005-6962-9

Schmitz, T.W., Mur, M., Aghourian, M., Bedard, M.-A., Spreng, R.N., 2018. Longitudinal Alzheimer's degeneration reflects the spatial topography of cholinergic basal forebrain projections. Cell Rep. 24 (1), 38–46. https://doi.org/10.1016/j.celrep.2018.06.001

Schmitz, T.W., Nathan Spreng, R., Weiner, M.W., Aisen, P., Petersen, R., Jack, C.R., The Alzheimer's Disease Neuroimaging I, 2016. Basal forebrain degeneration precedes and predicts the cortical spread of Alzheimer's pathology. Nat. Commun. 7 (1), 13249. https://doi.org/10.1038/ncomms13249

Schmitz, T.W., Zaborszky, L., 2021. Chapter 10 - Spatial topography of the basal forebrain cholinergic projections: organization and vulnerability to degeneration. In: Swaab, D.F., Kreier, F., Lucassen, P.J., Salehi, A., Buijs, R.M. (Eds.), Handbook of Clinical Neurology. Elsevier, Amsterdam, pp. 159–173.

Teipel, S., Heinsen, H., Amaro, E., Grinberg, L.T., Krause, B., Grothe, M., 2014. Cholinergic basal forebrain atrophy predicts amyloid burden in Alzheimer's disease. Neurobiol. Aging 35 (3), 482–491. https://doi.org/10.1016/j.neurobiolaging.2013.09.029

Teipel, S.J., Flatz, W.H., Heinsen, H., Bokde, A.L.W., Schoenberg, S.O., Stöckel, S., Dietrich, O., Reiser, M.F., Möller, H.-J., Hampel, H., 2005. Measurement of basal forebrain atrophy in Alzheimer's disease using MRI. Brain 128 (11), 2626–2644. https://doi.org/10.1093/brain/awh589

Vandenberghe, R., Van Laere, K., Ivanoiu, A., Salmon, E., Bastin, C., Triau, E., Hasselbalch, S., Law, I., Andersen, A., Korner, A., Minthon, L., Garraux, G., Nelissen, N., Bormans, G., Buckley, C., Owenius, R., Thurfjell, L., Farrar, G., Brooks, D.J., 2010. 18F-flutemetamol amyloid imaging in Alzheimer disease and mild cognitive impairment: a phase 2 trial. Ann. Neurol. 68 (3), 319–329. https://doi.org/10.1002/ana.22068

Villemagne, V.L., Burnham, S., Bourgeat, P., Brown, B., Ellis, K.A., Salvado, O., Szoeke, C., Macaulay, S.L., Martins, R., Maruff, P., Ames, D., Rowe, C.C., Masters, C.L., 2013. Amyloid β deposition, neurodegeneration, and cognitive decline in sporadic Alzheimer's disease: a prospective cohort study. Lancet Neurol. 12 (4), 357–367. https://doi.org/10.1016/S1474-4422(13)70044-9

Xia, Y., Eeles, E., Fripp, J., Pinsker, D., Thomas, P., Latter, M., Doré, V., Fazlollahi, A., Bourgeat, P., Villemagne, V.L., Coulson, E.J., Rose, S., 2022. Reduced cortical cholinergic innervation measured using [18F]-FEOBV PET imaging correlates with cognitive decline in mild cognitive impairment. NeuroImage Clin. 34, 102992. https://doi.org/10.1016/j.nicl.2022.102992

Zaborszky, L., Hoemke, L., Mohlberg, H., Schleicher, A., Amunts, K., Zilles, K., 2008. Stereotaxic probabilistic maps of the magnocellular cell groups in human basal forebrain. Neuroimage 42 (3), 1127–1141. https://doi.org/10.1016/j.neuroimage.2008.05.055